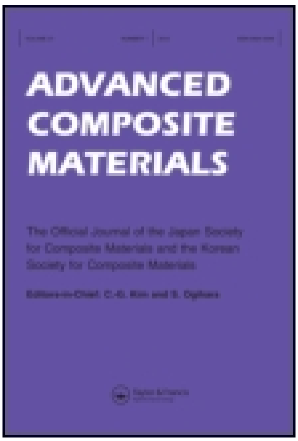

Advanced Composite Materials
Publication details, including instructions for authors and subscription information:
http://www.tandfonline.com/loi/tacm20

Damage detection of CFRP pipes and shells by using localized flexibility method

Yoshio Aoki & O-Il Byon (Goichi Ben)

Version of record first published: 02 Apr 2012.

Adv. Composite Mater., Vol. 10, No. 2,3, pp. 189–198 (2001)

Damage detection of CFRP pipes and shells by using localized flexibility method

YOSHIO AOKI [1] and O-IL BYON (GOICHI BEN) [2]

[1] *Department Precision Machinery Engineering, College of Science and Technology, Nihon University, 7-24-1 Narashinodai, Funabashi, Chiba, 274-8501 Japan*

[2] *Department of Mechanical Engineering, College of Industrial Technology, Nihon University, 1-2-1 Izumi-cho, Narashino, Chiba, 275-8575 Japan*

Abstract—This paper presents modal-based structural damage detection. Specifically, we focus on localized flexibility properties that can be deduced from the experimentally determined global flexibility matrix. We present the underlying theory that can be viewed as a generalized flexibility formulation in three different generalized coordinates, namely, localized or substructural displacement-basis, elemental deformation-basis and element strain-basis. Then, the present methods are applied to CFRP pipes and shells having interior damage and the numerical and experimental results show that the elemental strain-basis method is quite useful for detecting the damage inside CFRP filament winding pipes.

Keywords: CFRP; damage detection; localized flexibility; inverse problem; FEM filament winding.

1. INTRODUCTION

Among engineering materials, CFRP composites have very favorable strength and stiffness-to-weight ratios, which make their aerospace applications highly desirable, as weight savings translate directly into higher performance. A major concern in using these composites is their vulnerability to impulsive loading by space debris, pebbles and dusts. This is because crack or damage caused by interlaminar delaminations or fiber-matrix debonding in laminated composites, although not visible on the surface, significantly reduces their strength and/or stiffness. A rational method for the detection of damage location and damage modes or mechanisms in composites can therefore facilitate a wider acceptance of composites by practicing engineers.

To this end, several damage detection methods have been proposed, which include ultrasonic crack detection, wave propagation and scattering, modal testing, among others [1, 2]. We have applied the localized flexibility method to damage identification in CFRP laminated beam and have shown good agreement of analytical results with the experimental ones [3]. The objective of the present paper is to offer a model-based damage detection technique by relying on vibration test data. It should be mentioned that on-site vibration test is becoming economical and mobile as new miniaturized sensors of both contact and non-contact high-fidelity types which are readily available.

The present paper is organized as follows. First, a brief review of the variational formulation of the partitioned equations of motion for a vibrating structures is described. Second, by solving for the partitioned or substructural displacement, the relation between the partitioned flexibility and the global flexibility is established. The relation of the global frequency response function (FRF) to the partitioned FRF is then established by using the input/output invariance requirement. Third, by decomposing the elemental output displacement vector in terms of the strain amplitudes, a theory for strain output-based damage detection is derived by treating the strain gauge records. The damage location is estimated by the present three localized flexibility changes for CFRP filament winding pipes.

2. REVIEW OF LOCALIZED FLEXIBILITY FORMULATION

2.1. Global flexibility matrix

The discrete energy functional Π for a linear damped structure can be expressed as

$$\Pi(u_{\rm g}) = u_{\rm g}^{\rm T}\left(\frac{1}{2}K_{\rm g}u_{\rm g} - f_{\rm g}^{\rm D}\right),$$

$$K_{\rm g} = L^{\rm T}KL, \quad K = \begin{bmatrix} K^1 & & \\ & K^2 & \\ & & K^{n_{\rm s}} \end{bmatrix}, \quad f_{\rm g}^{\rm D} = f_{\rm g} - M_{\rm g}\ddot{u}_{\rm g} - C_{\rm g}\dot{u}_{\rm g}, \tag{1}$$

where $u_{\rm g}$ is the displacement vector of the assembled structure; $f_{\rm g}^{\rm D}$ is D'Alambert's force vector that consists of the applied force vector $f_{\rm g}$, the resisting inertia force $M_{\rm g}\ddot{u}_{\rm g}$, and the dissipating force $C_{\rm g}\dot{u}_{\rm g}$, $K_{\rm g}$ is the assembled stiffness matrix; $C_{\rm g}$ is the assembled damping matrix; $M_{\rm g}$ is the mass matrix of the assembled structure; K is the block diagonal collection of unassembled substructural stiffness matrices; L is the Boolean assembly matrix that relates the global and substructural displacements; the superscript $(\dot{})$ designates time differentiation, and the subscript (g) designates 'an assembled global structure' to distinguish from 'partitioned substructures'.

The discrete damped, time-invariant linear equations of motion for vibrating structures can be obtained from the stationary value of the preceding discrete energy functional, namely, $\delta\Pi = 0$:

$$M_{\rm g}\ddot{u}_{\rm g} + C_{\rm g}\dot{u}_{\rm g} + K_{\rm g}u_{\rm g} = f_{\rm g}. \tag{2}$$

The input-output relation, referred to as the *frequency response function* (FRF), is obtained by substituting a harmonic form of the input–output vectors as

$$\begin{bmatrix} u_g \\ f_g \end{bmatrix} = e^{j\omega t} \begin{bmatrix} \bar{u}_g \\ \bar{f}_g \end{bmatrix}, \tag{3}$$

and solving for the frequency-domain output $\bar{u}_g$:

$$\bar{u}_g = H_g(\omega)\bar{f}_g, \quad H_g(\omega) = \left(K_g + j\omega C_g - \omega^2 M_g\right)^{-1}, \tag{4}$$

where $H_g(\omega)$ is called the 'global' flexibility matrix and becomes $K_g^{-1}(= F_g)$ in the quasi-static limit ($\omega \rightarrow 0$). This matrix can be also obtained in terms of the eigenmodes Φ and eigenvalues Λ as

$$F_g = \Phi\Lambda^{-1}\Phi^T, \quad \Phi^T M_g \Phi = I, \quad \Phi^T K_g \Phi = \Lambda. \tag{5}$$

In practice, the size of the experimentally identified global flexibility matrix is given by

$$F_g = \Phi_m \Lambda_m^{-1} \Phi_m^T, \tag{6}$$

where the subscript (m) denotes the measured eigen values and modes which are substantially smaller than the analytical mode size.

2.2. *Substructural flexibility equation*

Since our objective is to identify the damage location and reduction of the rigidity, and the global flexibility-based damage indicators are known to be hidden localized damage attributes, we employ a general partitioned flexibility method presented by Park and Felippa [4] to relate the experimentally measured global flexibility matrix in equation (6) in terms of the corresponding localized flexibility matrices. This is accomplished as follows. First, a structure that is in equilibrium under applied forces is partitioned into substructures or elements. Hence, each of the partitioned substructures would be subject to the corresponding applied forces plus the Lagrange multipliers acting along the substructural partition interfaces. In order to maintain the kinematical compatibility along the partitioned boundaries, the displacement vector of the partitioned substructures u must satisfy the following relation:

$$u - Lu_g = 0, \tag{7}$$

where u represents the collection of all the substructural displacements. The element-by-element force vector f that is conjugate with the substrutural displacement is given by

$$L^T f = f_g, \tag{8}$$

so that the desired FRF must assume the following form:

$$\bar{u} = H(\omega)\bar{f}. \tag{9}$$

Observe that equation (9) relates the input $\bar{f}$ which is acting on each substructure defined in equation (8) to the output of individual substructural displacements $\bar{u}$ introduced in equation (7). Therefore, by introducing a Lagrange multiplier vector $\lambda_\ell$to enforce the kinematic compatibility condition equation (7), the system energy functional expressed in terms of the global nodal variables given in equation (1) is transformed into the three-variable functional:

$$\Pi(u, \lambda_\ell, u_{\mathrm{g}}) = u^{\mathrm{T}}\left(\frac{1}{2}Ku - f + M\ddot{u} + C\dot{u}\right) - \lambda_\ell^{\mathrm{T}} B^{\mathrm{T}}(u - Lu_{\mathrm{g}}), \tag{10}$$

where M and C are the substructural mass and damping matrices, and B is a constraint projection matrix that extracts the partition boundary substructural nodes. The stationary value of the above functional leads to the following equations of motion for partitioned structures:

$$\begin{bmatrix} \ddot{M} + \dot{C} + K & -B & 0 \\ -B^{\mathrm{T}} & 0 & L_{\mathrm{b}} \\ 0 & L_{\mathrm{b}}^{\mathrm{T}} & 0 \end{bmatrix} \begin{Bmatrix} u \\ \lambda_\ell \\ u_{\mathrm{g}} \end{Bmatrix} = \begin{Bmatrix} f \\ 0 \\ 0 \end{Bmatrix}, \quad L_{\mathrm{b}} = B^{\mathrm{T}} L. \tag{11}$$

The substructure-by-substructure FRF that we seek can now be obtained from equation (11) as

$$\begin{aligned} H(\omega) &= H_{\mathrm{e}}(\omega)\big\{I - BK_{\mathrm{B}}(\omega)\big[I - L_{\mathrm{b}}H_{\mathrm{L}}(\omega)L_{\mathrm{b}}^{\mathrm{T}}K_{\mathrm{B}}(\omega)\big]B^{\mathrm{T}}H_{\mathrm{e}}(\omega)\big\}, \qquad (12)\\ H_{\mathrm{e}}(\omega) &= \big(K + j\omega C - \omega^2 M\big)^{-1}, \quad K_{\mathrm{B}}(\omega) = \big(B^{\mathrm{T}}H_{\mathrm{e}}(\omega)B\big)^{-1}, \\ H_{\mathrm{L}}(\omega) &= \big(L_{\mathrm{b}}^{\mathrm{T}}K_{\mathrm{B}}(\omega)L_{\mathrm{b}}\big)^{-1}. \end{aligned}$$

It can be shown that the substructural FRF $H(\omega)$ can also be obtained in terms of the global FRF $H_{\mathrm{g}}(\omega)$, namely,

$$H(\omega) = LH_{\mathrm{g}}(\omega)L^{\mathrm{T}} = L\big(K_{\mathrm{g}} + j\omega C_{\mathrm{g}} - \omega^2 M_{\mathrm{g}}\big)^{-1}L^{\mathrm{T}}. \tag{13}$$

Observe that the substructural FRF given by equation (12) reveals the substructural compositions consisting of the substructural mass, damping and stiffness matrices. On the other hand, the same FRF obtained by the input/output invariance property given by equation (13) masks the substructural compositions, showing only the global quantities. Their combined use leads to an important application in detecting damages as shown below. For the quasistatic limit (i.e. $\omega \to 0$), the two expressions provide the following Ricatti-like equation:

$$\begin{aligned} LF_{\mathrm{g}}L^{\mathrm{T}} &= F\big\{I - BF_{\mathrm{B}}^{-1}\big[I - L_{\mathrm{b}}F_{\mathrm{L}}L_{\mathrm{b}}^{\mathrm{T}}F_{\mathrm{B}}^{-1}\big]B^{\mathrm{T}}F\big\}, \\ F &= K^{-1},\ F_{\mathrm{B}} = (B^{\mathrm{T}}FB),\ F_{\mathrm{L}} = \big(L_{\mathrm{b}}^{\mathrm{T}}F_{\mathrm{B}}^{-1}L_{\mathrm{b}}\big)^{-1}. \end{aligned} \tag{14}$$

where F is called the substructural flexibility matrix of block diagonal form.

2.3. Deformation-basis flexibilities

The substructural flexibility matrix $\mathrm{F} = \mathrm{K}^{-1}$ given in equation (14) consists of both free-free deformation modes plus the rigid body modes. This poses no difficulty when the experimentally identified global flexibility F_g in equation (6) is a full basis matrix, that is, the eigenvector Φ_m is a square matrix. In practice, the measured modes (m) are often a fraction of the sensor output numbers (s), namely, for Φ_m, $s > m$. This observation motivated us to transform the free-free substructural flexibility matrix F into a constrained deformation flexibility which can lead to a sharper indication of damage. Let us decompose the substructural displacements u further into deformational and rigid parts:

$$u = d + R\alpha, \tag{15}$$

where d is the deformational part, R describes the substructural rigid-mode shapes, and α represents the rigid-mode amplitudes. In order to eliminate the rigid-body motions from the substructural displacements, we partition equation (15) according to:

$$\begin{Bmatrix} u_c \\ u_f \end{Bmatrix} = \begin{Bmatrix} d_c \\ d_f \end{Bmatrix} + \begin{Bmatrix} R_c \\ R_f \end{Bmatrix} \alpha, \quad R = \begin{bmatrix} R^1 & & & \\ & R^2 & & \\ & & \cdot & \\ & & & R^{n_s} \end{bmatrix}, \tag{16}$$

where R_c is a square invertible submatrix corresponding to 'temporarily constrained nodes' and R_f refers to unconstrained nodes. Hence, R_c would be a (3×3) matrix. Similarly, the constrained-node rigid-body amplitudes R_c for other substructural cases can be chosen. Solving for α from the first row of equation (16), we obtain

$$\alpha = R_c^{-1}(u_c - d_c). \tag{17}$$

We now introduce a deformation measure that represents deformations at nodes f with respect to nodes c:

$$v = d_f - R_f R_c^{-1} d_c = Tu = TLu_g, \quad T = [-\overline{R}\ I], \quad \overline{R} = R_f R_c^{-1}. \tag{18}$$

Using this relation, its conjugate force vectors are given by

$$T^T f_v = f \Rightarrow L^T T^T f_v = L^T f = f_g. \tag{19}$$

The variational functional equation (10) expressed in terms of the substructural displacement u is transformed into that of the deformation variable v, which in the quasi-static limit becomes:

$$\Pi(v, \lambda_v, u_g) = v^T\left(\frac{1}{2}K_v v - f_v\right) - \lambda_v^T B_v^T (v - TLu_g), \quad K = T^T K_v T. \tag{20}$$

A simple expression is obtained if the constraint operator B_{v} is chosen as a nullspace of TL, namely,

$$B_{\mathrm{v}}^{\mathrm{T}}(TL) = 0. \tag{21}$$

So the stationary condition $\delta\Pi = 0$ of equation (20) yields

$$\begin{bmatrix} K_{\mathrm{v}} & -B_{\mathrm{v}} \\ -B_{\mathrm{v}}^{\mathrm{T}} & 0 \end{bmatrix} \begin{Bmatrix} v \\ \lambda_{\mathrm{v}} \end{Bmatrix} = \begin{Bmatrix} f_{\mathrm{v}} \\ 0 \end{Bmatrix}, \tag{22}$$

which will be called the deformational quasi-static equations of motion for partitioned structures. A Riccati-like equation which relates the global flexibility to the deformation-basis substructural flexibility can be obtained in a similar manner as for the substructural displacement case, equation (14):

$$TLF_{\mathrm{g}}L^{\mathrm{T}}T^{\mathrm{T}} = P_{\mathrm{v}}^{\mathrm{T}}F_{\mathrm{v}}P_{\mathrm{v}}, \quad F_{\mathrm{v}} = K_{\mathrm{v}}^{-1}, \quad P_{\mathrm{v}} = I - B_{\mathrm{v}}\left[B_{\mathrm{v}}^{\mathrm{T}}F_{\mathrm{v}}B_{\mathrm{v}}\right]^{-1}B_{\mathrm{v}}^{\mathrm{T}}F_{\mathrm{v}}. \tag{23}$$

2.4. *Strain-basis flexibilities*

We have experienced that the use of the deformational flexibilities F_{v} yields an adequate identification of damage locations. In many applications not only identifying damage locations but also damage mechanisms are equally important. For only through understanding damage mechanisms can one develop damage prevention measures. An effective approach to detect damage mechanisms is to utilize strain-basis substructural flexibilities. As an example, a typical substructure consists of membrane, transverse shear and bending strains. By identifying which of the three strains undergo a major strain change, one may deduce the damage mechanisms. The necessary transformation to obtain strain-basis flexibilities is shown below. Let us assume that the strain output s can be related to the substructural displacement u according to

$$s = Du = DLu_{\mathrm{g}}, \tag{24}$$

where D is the discrete strain-displacement relation matrix that can be derived in a variety of ways, for example, by relying on the finite element shape functions. With this change of basis, one arrives at the following strain-basis functional and the corresponding equations of motion in quasi-static form:

$$\Pi(s, \lambda_{\mathrm{s}}) = s^{\mathrm{T}}\left(\frac{1}{2}K_{\mathrm{s}}s - f_{\mathrm{s}}\right) - \lambda_{\mathrm{s}}^{\mathrm{T}}B_{\mathrm{s}}^{\mathrm{T}}(s - DLu_{\mathrm{g}}), \quad K = D^{\mathrm{T}}K_{\mathrm{s}}D, \; B_{\mathrm{s}}^{\mathrm{T}}(DL) = 0, \tag{25}$$

$$L^{\mathrm{T}}D^{\mathrm{T}}f_{\mathrm{s}} = f_{\mathrm{g}} \Rightarrow \begin{bmatrix} K_{\mathrm{s}} & -B_{\mathrm{s}} \\ -B_{\mathrm{s}}^{\mathrm{T}} & 0 \end{bmatrix} \begin{Bmatrix} s \\ \lambda_{\mathrm{s}} \end{Bmatrix} = \begin{Bmatrix} f_{\mathrm{s}} \\ 0 \end{Bmatrix}.$$

The global flexibility F_{g} is then related to the strain-basis substructural flexibility F_{s} according to:

$$DLF_{\mathrm{g}}L^{\mathrm{T}}D^{\mathrm{T}} = P_{\mathrm{s}}^{\mathrm{T}}F_{\mathrm{s}}P_{\mathrm{s}}, \quad F_{\mathrm{s}} = K_{\mathrm{s}}^{-1}, \quad P_{\mathrm{s}} = I - B_{\mathrm{s}}\left[B_{\mathrm{s}}^{\mathrm{T}}F_{\mathrm{s}}B_{\mathrm{s}}\right]^{-1}B_{\mathrm{s}}^{\mathrm{T}}F_{\mathrm{s}}, \tag{26}$$

which can be used not only for localized damage detection but more importantly for identifying damage mechanisms.

3. APPLICATIONS TO DAMAGE DETECTION IN CONTINUUM CFRP COMPOSITES

To illustrate the applicability to continuum composites of the localized damage detection techniques reviewed in the preceding sections, we first evaluate the methods for analytical problems. Validation of the damage detection methods by the experimental data then follows.

3.1. Analytical demonstration

In order to demonstrate the validity of the present method, a CFRP filament winding pipe having 34 mm diameter, length of 500 mm, 2 mm thickness, winding angle of 45° and clamped at the both ends is chosen as an example. The pipe is divided into 12 beam elements in the FEM analysis and the bending rigidity of the 6th element is assumed to have a value 80% of that of other elements owing to the damage. To asess the relative performance of three methods, the global flexibility F_{g} is adopted as an inverse of the global stiffness matrix that is obtained from the corresponding FEM analysis. A homotopy iterative procedure [5] is then used to obtain the free-free substructural flexibility F given in equation (14), the deformation-basis flexibility F_{v} in equation (23) and the strain-basis flexibility F_{s} in equation (26). For damage detection we have employed the change of rigidity ratio δ:

$$\delta^{\mathrm{ns}} = \mathrm{diag}\left(F^{\mathrm{ns}}_{\mathrm{damage}} - F^{\mathrm{ns}}_{\mathrm{healthy}}\right)/F^{\mathrm{ns}}_{\mathrm{damage}} = K^{\mathrm{ns}}_{\mathrm{damage}} - K^{\mathrm{ns}}_{\mathrm{healthy}}/K^{\mathrm{ns}}_{\mathrm{healthy}}, \qquad (27)$$

where the superscript (ns) designates the substructural component or degree of freedom.

In Figs 2–4, the solid line indicates the change of rigidity ratio calculated by using the 44 eigenvalues and eigenvectors in the global flexibility matrix F_{g} and the broken line with asterisks (*) is the change of rigidity ratio calculated by using only the first three eigen values and modes in the F_{g}. When the free-free substructural flexibility method is used, the damage is detected at the degree of freedom from 19

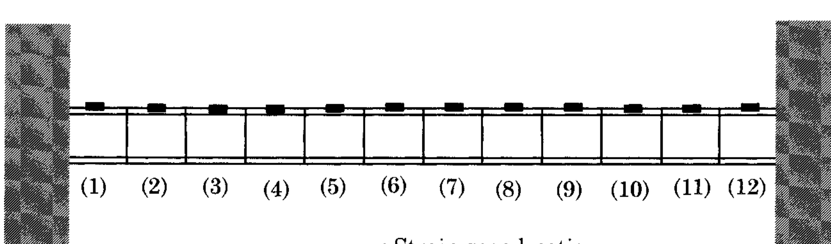

Figure 1. Partition elements and the location of the strain gage.

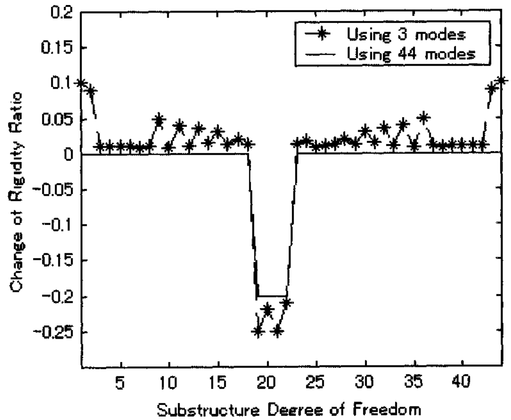

Figure 2. Damage detection based on substructural flexibility.

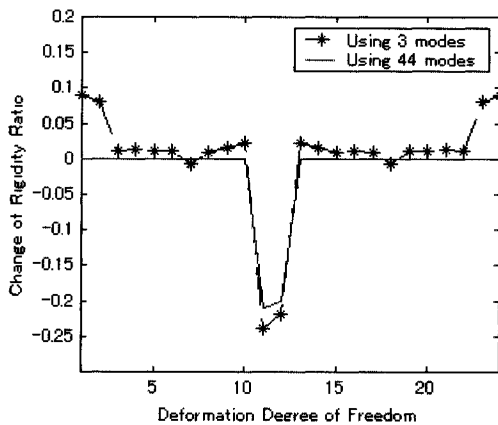

Figure 3. Damage detection based on deformation flexibility.

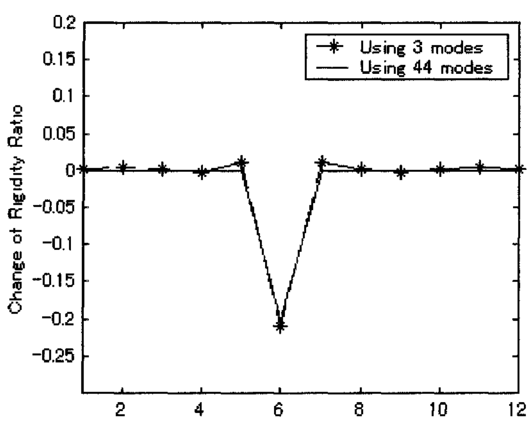

Figure 4. Damage detection based on strain flexibility.

to 22 corresponding to the 6th element, as shown in Fig. 2. The resulting rigidity ratio as solid line provides the location of damage correctly and the rigidity ratio of the corresponding element shows the assumed value of −0.2. Since only the first three eigenvalues and modes are used for calculating the global flexibility F_g in equation (6), the change of rigidity ratio as broken line (*) cannot be accurately computed. Nevertheless, the location of damaged elements is correctly determined. As for the deformation-based flexibility method, the damage should occur at the degree of freedoms 11 and 12, as shown in Fig. 3. Both results correctly trace, except the 11th and 12th degrees of freedom, but their values are overestimated somewhat for the assumed reduced bending rigidity. Finally, Fig. 4 shows that the damage indication based on the strain-basis flexibilities not only correctly detects the damaged 6th element but also computes almost the same rigidity ratio of −0.2. So far as the identification in CFRP filament winding pipe is concerned, the strain-basis damage indication can predict it well within acceptable accuracy ranges.

3.2. Application to experimental data

We have carried out the damage detection procedure for experimental strain data obtained on the CFRP filament winding pipe mentioned before. The strain data have been measured at the center of the twelve elements on the CFRP pipe specimens as shown in Fig. 1. The 6th element of pipe specimen has 50% bending rigidity ratio compared with the other elements. This bending rigidity reduction has been realized by cutting out a half of the cross-section area and this area is extended over a half of the circumferential length. The CFRP pipe has then been subjected to forced vibration tests under sinusoidal signal from 10 Hz to 1200 Hz. The frequency response functions (FRFs) have been obtained by using a Fast Fourier Transform analyzer and the strains are measured for the first three eigenmodes of healthy and damaged specimens. By using the experimentally determined three global flexibility modes, the rigidity ratios based on the strain-basis flexibility changes are computed and shown in Fig. 5. By comparing the experimental case shown in Fig. 5 with the analytical case (see Fig. 4), it is seen that the damage locations are correctly determined. The bending rigidity of the damaged element is overestimated for the real test case, but is well within acceptable accuracy ranges.

4. CONCLUSIONS

The change of rigidity ratio that utilizes the three localized flexibilities has been applied to the damage detection of CFRP composite pipes and shells. The free-free localized flexibility and the deformation-basis flexibilities can make use of conventional output data, such as acceleration or displacement. The strain-basis localized flexibility can utilize a combination of the conventional modal testy output as well as the strain output. Then, the damage detection of CFRP filament winding pipe has been carried out by using strain gage records. The main features of the present study are summarized as follows.

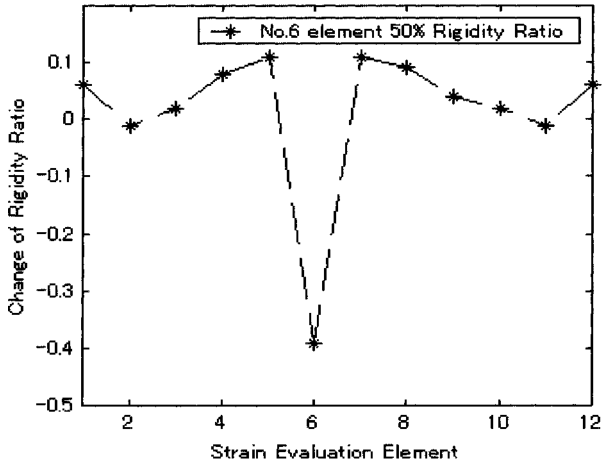

Figure 5. Experimental damage detection based on strain flexibility.

(1) The relative accuracy fidelities of the three localized flexibilities are evaluated as applied to the damage detection of CFRP composite pipes analytically. All three flexibility methods accurately captured the locations of rigidity changes. Among the three, the strain-basis flexibility method is most accurate.

(2) By using the global flexibility of CFRP filament winding pipes determined by the first three strain eigenmodes, damage detection are carried out by the strain-basis flexibility method. The result demonstrates that damage location is identified with high confidence as well as reasonably accurate change in the bending rigidity.

REFERENCES

1. S. W. Doebling *et al.*, Damage identification and health monitoring of structural and mechanical system from changes in their vibration characteristics: a literature survey, Los Alamos National Laboratory, Report No. LA-12767-MS, Los Alamos, NM (1996).
2. K. C. Park, G. W. Reich and K. F. Alvin, Damage detection using localized flexibilities, in: *Structural Health Monitoring, Current Status and Perspectives*, F. K. Chang (Ed.), pp. 125–139. Technomic Publishers (1997).
3. O. I. Byon, Y. Aoki, T. Yamaguchi and K. C. Park, Damage detection of CFRP laminates composites by localized flexibility method, in: *Proceedings of 12th International Conference on Composite Materials*, p. 375 (1999).
4. K. C. Park and C. A. Felippa, A variational framework for solution method developments in structural mechanics, *J. Appl. Mech.* **65** (1), 242–249 (1998).
5. S. L. Richter and E. G. Collins, Jr., A homotopy algorithm for reduced-order controller design using the optimal projection equations, in: *Proceedings of the Conference on Decision and Control*, pp. 331–338 (1989).